Pure Appl. Chem., Vol. 72, No. 12, pp. 2319–2332, 2000.

Concepts of metal-mediated methane functionalization. An intersection of experiment and theory*,†

Helmut Schwarz‡ and Detlef Schröder

Institut für Organische Chemie der Technischen Universität Berlin, Straße des 17. Juni 135, D-10623 Berlin, Germany

Abstract: Concepts for the activation of methane are derived from ion-molecule reactions of mass-selected, ground-state transition-metal cations M^+. Elementary steps of industrially important processes are uncovered (e.g., oxygenation of methane or its coupling with carbon dioxide). In addition, the implications of the electronic structures of $M(CH_2)^+$ complexes for their reactions with nucleophiles are discussed, and the crucial role of contemporary quantum mechanical calculations in the elucidation of mechanistic details is emphasized.

INTRODUCTION

The transition-metal-mediated functionalization of methane constitutes an important, timely topic of research stimulated by both the challenging inertness of this simplest hydrocarbon molecule and the substantial economic interest in the use of natural gas resources [1–6]. Insights into the role of the electronic structure of the metals [7] and the mechanistic details of the activation process can be gained by studies of mass-selected metal ions in the gas phase. This approach allows to unravel the intrinsic chemical behavior of metals at a molecular level under rigorous exclusion of many complicating factors such as solvent and aggregation effects, counterions or ligands. Not surprisingly, methane activation by bare ("naked") transition-metal cations M^+ has been at the focus of a number of fundamental gas-phase ion studies [7,8]. While several electronically excited ions were reported to dehydrogenate methane (Reaction 1) and to form metal-carbene complexes $M(CH_2)^+$ [9,10], thermalized ground-state monoatomic 3d- and 4d-transition-metal cations do not react with methane [7,11–15].

$$CH_4 + M^+ \longrightarrow H_2 + M(CH_2)^+ \quad (1)$$

This unreactivity of bare metal ions, especially from the first row, is due to properties of the occupied 4s orbital [7] and unfavourable thermodynamics. To make Reaction 1 thermochemically feasible, the metal-methylidene bond strength $D_0(M^+–CH_2)$ has to exceed 111 kcal/mol, i.e., the dissociation energy of CH_4 to CH_2 and H_2. Irikura and Beauchamp were the first who discovered that bare third-row transition-metal cations M^+ (M = Ta, W, Os, Ir, Pt) dehydrogenate methane in a stoichiometric manner to yield $M(CH_2)^+$ [20–22]. In these cases, Reaction 1 is driven by the formation of extraordinarily strong metal-carbene bonds, and these remarkable bond strengths can be attributed to relativistic stabilization of the cationic complexes $M(CH_2)^+$ [23] as demonstrated by fully relativistic four-component Dirac–Fock Coulomb benchmark calculations including correlation effects [24]. The reactions of Ir^+

*Plenary lecture presented at the 15th International Conference on Physical Organic Chemistry (ICPOC 15), Göteborg, Sweden, 8–13 July 2000. Other presentations are published in this issue, pp. 2219–2358.

†This article is dedicated to the memory of the late Prof. Ben S. Freiser, Purdue University, who has pioneered the field of organometallic gas-phase ion chemistry. Plenary lectures given by H. S. as the IUPAC Conferences on Physical Organic Chemistry (Göteborg, Sweden, 8–13 July 2000) and on Chemical Thermodynamics (Halifax, Nova Scotia, 6–11 2000) were based on the material presented here.

‡Corresponding author: Fax: ++49 30 314 21102; E-mail: schw0531@www.chem.tu-berlin.de

[14,25], Pt^+ [26–29], and other transition-metal cations M^+ with methane have also formed the subject of detailed theoretical investigations using different levels of theory [30–34].

In this account, an overview will be given on the gas-phase reactions of several $M(CH_2)^+$ complexes with molecular oxygen, carbon dioxide, and various nucleophiles aimed at uncovering the intrinsic mechanistic details of these extremely important coupling reactions by which, *inter alia*, methane is converted to CH_3OH, CH_2O, CH_3CO_2H, HCN, and other C-heteroatom coupling products. In addition, recent results for a direct amination of methane ($CH_4 \rightarrow CH_3NH_2$) as well as a new paradigm in the oxidation of CH_4 (and other hydrocarbons) by bare binary metal-oxide cations MO^+ will be presented. We will refrain from presenting any experimental and computational details; they can be found in the references given as well as in several review articles on gas-phase metal-ion chemistry [7,12,35–37].

GAS-PHASE REACTIONS OF $M(CH_2)^+$

Oxidation of $Pt(CH_2)^+$ with molecular oxygen

The discovery [38] that bare Pt^+, in an unprecedented manner, catalyzes partial oxidation of methane by molecular oxygen to methanol, formaldehyde, and higher oxidation products (Scheme 1) has generated quite some interest. A key intermediate in the catalytic cycle is the carbene $Pt(CH_2)^+$, which is formed according to Reaction 1 with an efficiency ϕ = 0.8 [39]. This cationic carbene reacts with molecular oxygen to atomic Pt^+ (70%) via liberation of neutral $[C,H_2O_2]$. In a parallel channel, PtO^+ and CH_2O are formed (30%), and PtO^+ then serves as an efficient oxidant of CH_4 to produce in competition the couples $Pt(CH_2)^+/H_2O$ (75%) and Pt^+/CH_3OH (25%). Mechanistic insight in this complicated reaction sequence was provided by detailed electronic structure calculations including relativistic and spin-orbit effects [28]. While some of the steps depicted in Scheme 1 correspond to well-known mechanisms, e.g., oxidative addition, reductive elimination, or hydrogen transfer, some less common types of reactions are also involved. The most notable reaction concerns the key step in the overall catalytic cycle, i.e., the reaction of $Pt(CH_2)^+$ with O_2. While this oxidation process involves as a central intermediate a four-numbered metallacycle, which is formed by a formal [2 + 2] addition of O_2 to $Pt(CH_2)^+$, the reaction mechanism must not be confused with a metathesis process. Rather, the compu-

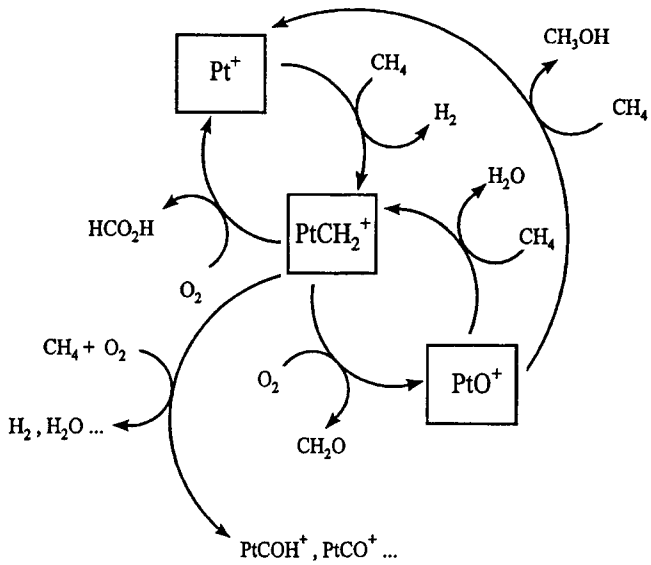

Scheme 1 Catalytic methane oxidation by atomic Pt^+ and molecular oxygen (taken from ref. 38).

tations reveal a complicated potential-energy surface, and at least four discrete minima are involved on the way from $Pt(CH_2)^+/O_2$ to PtO^+/CH_2O [28].

Tantalum-mediated coupling of methane and carbon dioxide via $Ta(CH_2)^+$

Selectivity in the C–H bond activation of alkanes has been referred to as the chemists' Holy Grail [41]. Clearly, an even greater challenge due to inherent thermochemical and kinetic obstacles concerns the simultaneous coupling of alkanes with CO_2 to yield the corresponding carboxylic acids (Reaction 2). Formation of acetic acid from CH_4 and CO_2, for example, is of particular importance, and this reaction is endergonic under standard conditions and even 9 kcal/mol endothermic in the gas phase, not to consider any possible barriers associated with the bond activation and coupling steps.

$$RH + CO_2 \xrightarrow{[M]} RCO_2H \quad (2)$$

With regard to a metal-mediated realization of Reaction 2 there are several prerequisites to be fulfilled by the metal [M]: it has to be capable of activating both CH_4 and CO_2; further, coupling of the fragments coordinated to the metal has to be brought about followed by product release to regenerate the metal catalyst. So far, the success obtained is disappointingly small. However, with regard to the realization of at least some elementary steps in the coupling of CH_4 and CO_2, a stoichiometric variant was found when bare Ta^+ was used [42]. While Ta^+ efficiently reduces CO_2 to generate TaO^+ and TaO_2^+, in contrast to many late transition-metal oxides [36] neither TaO^+ nor TaO_2^+ activate CH_4 in the gas phase. However, the carbene $Ta(CH_2)^+$, which forms efficiently from CH_4 and Ta^+ [13,20–22,26,38], is able to deoxygenate CO_2 rapidly ($\phi > 0.95$) to yield CO and $OTa(CH_2)^+$. The latter reacts slowly ($\phi = 0.2$) with a further equivalent of CO_2 to yield the dioxocation TaO_2^+ as the only product. Based on thermochemical and mechanistic considerations, the neutral C_2H_2O product formed in this reaction corresponds to ketene. The sequence of Reactions 3–5 demonstrates that, at a molecular level, coupling of CH_4 and CO_2 can be achieved (Reaction 6). Nevertheless, Ta^+ has to be used in stoichiometric amounts and is consumed as TaO_2^+. While the formation of strong tantalum–oxygen bonds is, on the one hand, the driving force for ketene generation, on the other hand the fact that TaO_2^+ cannot be reduced to Ta^+ by any of the common reagents limits the scope of the reaction. As to the elementary steps and the mechanism operative in this system, computational work by Sändig and Koch was extremely insightful [43,44]. For example, in contrast to the Pt^+/CH_4 couple [23,24,28,29] dehydrogenation of CH_4 by Ta^+ (Reaction 3) does not proceed adiabatically on one potential-energy surface; rather, along the reaction coordinate there are several changes in spin multiplicity. In contrast to the oxidation of $Pt(CH_2)^+$ with O_2 (see above), a genuine metathesis process is operative in the actual coupling step to generate ketene (Reaction 5), as was originally suggested [42].

$$CH_4 + Ta^+ \longrightarrow Ta(CH_2)^+ + H_2 \quad (3)$$

$$CO_2 + Ta(CH_2)^+ \longrightarrow OTa(CH_2)^+ + CO \quad (4)$$

$$CO_2 + OTa(CH_2)^+ \longrightarrow TaO_2^+ + C_2H_2O \quad (5)$$

$$CH_4 + 2CO_2 + Ta^+ \longrightarrow TaO_2^+ + H_2 + CO + C_2H_2O \quad (6)$$

Platinum-mediated coupling of methane and small nucleophiles: Models for C–N, C–O, C–P, and C–S bond formation

Here, we focus on the systems $Pt^+/CH_4/NH_3$ and $Pt^+/CH_4/H_2O$. Reactions with other nucleophiles (e.g., PH_3, H_2S, CH_3NH_2, and CH_3OH) are mentioned only briefly. Common intermediate in all systems is

the cationic platinum carbene $Pt(CH_2)^+$. Experimental details, including thermochemical, kinetic, computational, and labeling data, can be found in the original literature [45–47]. The chapter concludes with a comparison of Pt^+ with a series of selected 3d-, 4d-, and 5d-transition-metal cations; evidence is presented for the unique role of Pt^+ with respect both to activating CH_4 and to mediate efficient C–N bond coupling with NH_3.

$Pt(CH_2)^+$ reacts rapidly (ϕ = 0.3) with NH_3 under formation of $CH_2NH_2^+$, $PtC(H)NH_2^+$, and NH_4^+ (Reaction 7)

$$Pt(CH_2)^+ + NH_3 \xrightarrow{\begin{array}{l}70\%\\25\%\\5\%\end{array}} \begin{array}{l}CH_2NH_2^+ + PtH\\PtC(H)NH_2^+ + H_2\\NH_4^+ + PtCH\end{array} \qquad (7)$$

Whereas formation of NH_4^+ is a simple acid-base reaction, C–N bond coupling is achieved in the two other channels. The major pathway, to produce $CH_2NH_2^+$, is found to be exothermic by 23 kcal/mol (relative to the separated reactants $Pt(CH_2)^+/NH_3$), and all stationary points of the potential-energy surface are located below the entrance channel. The second pathway involves dehydrogenation to yield the aminocarbene complex $PtC(H)NH_2^+$ ($\Delta_r H$ = –36 kcal/mol). As to the mechanistic details, there are three options in the generation of $CH_2NH_2^+$ and PtH. Energetically most favored is a pathway commencing with a Pt^+-mediated N–H bond activation of the organometallic ion $PtCH_2NH_3^+$, followed by activation of a C–H bond of the methylene group and eventual liberation of H_2. Much less favored (but still below the energy of the entrance channel) is a reversed sequence in which a 1,2 hydrogen shift from carbon to platinum precedes the 1,3-hydrogen migration from N to Pt. While in these two paths platinum is involved directly and exploited as a catalyst, the direct 1,2-elimination of molecular hydrogen across the C–N unit, a process in which the metal only serves as a spectator, is 23 kcal/mol above the energy of the reactants (Scheme 2) and can thus be discounted.

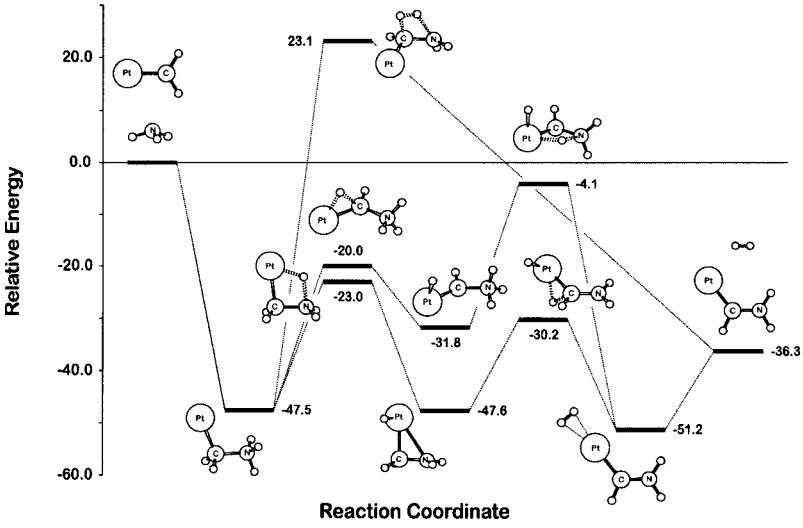

Scheme 2 PES for the dehydrogenation of $Pt(CH_2)^+/NH_3$ to yield $PtC(H)NH_2^+$ at the B3LYP/TZP//B3LYP/DZP level including corrections for zero-point vibrational energies; charges are omitted and energies given in kcal/mol (taken from ref. 47).

Despite some similarities, there are distinct differences in the reaction of $Pt(CH_2)^+$ with H_2O in comparison with the $Pt^+(CH_2)^+/NH_3$ system. For example, the efficiency of reaction 8 is very low (ϕ = 0.002). The initially formed platinum hydroxycarbene complex $PtC(H)OH^+$ is generated in only small stationary concentration due to a fast consecutive process with water to yield H_2 and $(H_2O)Pt(CO)^+$ (Reaction 9). Thus, the combined reactions of $Pt(CH_2)^+$ formed from Pt^+/CH_4 with two molecules of water to yield $(H_2O)Pt(CO)^+$ constitutes a gas-phase model for the platinum-mediated generation of water gas according to Scheme 3.

$$Pt(CH_2)^+ + H_2O \xrightarrow{5\%} Pt(CO)^+ + 2H_2 \quad (8)$$
$$\xrightarrow{95\%} PtC(H)OH^+ + H_2$$

$$PtC(H)OH^+ + H_2O \longrightarrow (H_2O)Pt(CO)^+ + H_2 \quad (9)$$

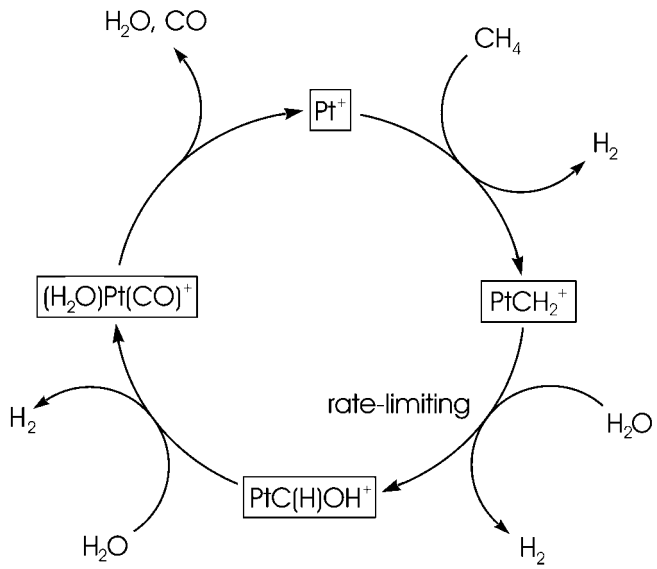

Scheme 3 Gas-phase model for the Pt^+-mediated conversion of CH_4 and H_2O into CO and H_2 (taken from ref. 45).

Interestingly, it is not the activation of methane but the addition of H_2O to $Pt(CH_2)^+$ that constitutes the rate-determining step in the sequence to produce $(H_2O)Pt(CO)^+$ (Scheme 3). As thermalized ions undergo only exothermic or almost thermoneutral reactions in gas-phase experiments of the type described here, the reaction stops after exothermic formation of $(H_2O)Pt(CO)^+$ because according to thermochemical estimates, the final ligand detachment of CO and H_2O has to be induced by an external input of about 102 kcal/mol to regenerate the bare Pt^+ [28].

In the reaction of $Pt(CH_2)^+$ with PH_3 (ϕ = 0.62), the third-row congener of ammonia, the major product (65%) corresponds to $Pt(PH)^+$ and CH_4. Compared to NH_3, the differences in product distributions can be ascribed to two major factors: (i) Due to the lower basicity of PH_3 (compared to NH_3) and (ii) less favorable π-bonding of phosporus, the formations of PH_4^+ and $CH_2PH_2^+$ are not observed. Interestingly, the main primary product $Pt(PH)^+$ reacts consecutively with excess PH_3 to yield $[Pt,P_mH_n]$ (m = 1–6; n = 0–3). Saturation is achieved after addition of six phosphorus atoms, and, based on cir-

cumstantial evidence, these clusters are suggested to contain P_2-building blocks, rather than intact P_4 or P_6 units [48].

Demethanation is also the major product (70%) in the reaction of $Pt(CH_2)^+$ with H_2S (ϕ = 0.32); $Pt(CS)^+$ and $Pt(CH_2S)^+$ are formed each with 15%. Consecutive dehydrogenative coupling reactions of PtS^+ with H_2S do also take place; however, for sulfur saturation is achieved for $Pt(S_4)^+$, and interesting speculations have been put forward aimed at correlating the maximum number of ligands n_{max} at Pt with the electronegativities of the elements and their abilitiy to form element–element bonds: n_{max} corresponds to 2 for oxygen, 4 for sulfur, 6 for phosphorus, and can be as large as 13 for silicon-containing fragments.

For the organic nucleophiles CH_3NH_2 and CH_3OH, the homologs of NH_3 and H_2O, C–N and C–O couplings are much less efficient than platinum-mediated C–H bond activation of the substrates. For example, the major primary process (40%) in the reaction of $Pt(CH_2)^+$ with CH_3NH_2 (ϕ = 0.4), is a hydride transfer from methylamine to the platinum–carbene cation to generate $CH_2NH_2^+$ and neutral $Pt(CH_3)$ and/or $HPt(CH_2)$. In contrast, this hydride transfer is negligible (2%) in the related $Pt(CH_2)^+/CH_3OH$ couple (ϕ = 0.24) and the dominant product is due to demethanation (63%). Extensive labeling experiments demonstrate convincingly that the demethanation product $[Pt,C,H_2,O]^+$ is formed via transfer of two hydrogen atoms from the methyl group of CH_3OH to the carbene unit of $Pt(CH_2)^+$. Thus, nucleophilic attack of methanol to the platinum carbene is negligible.

A pivotal question is whether the gas-phase process of metal-mediated carbon–nitrogen coupling (Reaction 7) in the functionalization of methane is confined to platinum, or if other metal cations also mediate C–N bond formation (Reaction 10). Therefore, the extension of this concept to other transition metals has been explored for selected 3d-, 4d-, and 5d-elements [47]. The product distributions of the reactions of $M(CH_2)^+$ and NH_3 are given in Table 1.

$$M^+ \xrightarrow{CH_4} M(CH_2)^+ \xrightarrow{NH_3} \text{C–N coupling products} \qquad (10)$$

The carbenes of the 3d-metals Fe^+ and Co^+ are unreactive toward ammonia. This inertness cannot be rationalized by the related metal–carbene bond strengths, as the carbenes of the 5d-homologs of

Table 1 Reaction efficiencies (ϕ_{NH_3})[a] and product-branching ratios[b] for the reactions of cationic transition-metal carbenes[c] with ammonia, and relative efficiencies for methane/ammonia coupling[d] with $\phi_{rel}(Pt) = 100$.

		Ionic reaction products[b]				
$M(CH_2)^+$	ϕ_{NH_3}[a]	NH_4^+	$CH_2NH_2^+$	M^+	$MC(H)NH_2^+$	ϕrel[d]
$Fe(CH_2)^+$	0.0[e]					0
$Co(CH_2)^+$	0.0[e]					0
$Rh(CH_2)^+$	0.1			75	25	0
$W(CH_2)^+$	0.1				100	6
$Os(CH_2)^+$	0.2	45			55	19
$Ir(CH_2)^+$	0.4	60			40	65
$Pt(CH_2)^+$	0.3	5	70		25	100
$Au(CH_2)^+$	0.6		100			0

[a]Given as $\phi = k_r/k_c$.

[b]Branching ratios normalized to a sum of 100%.

[c]The following precursor systems were used to generate the metal carbene cations: $Fe^+/C_2H_4/N_2O$; Co^+/C_7H_8; $Rh^+/c\text{-}C_3H_6$; W^+/CH_4; Os^+/CH_4; Ir^+/CH_4; Pt^+/CH_4; Au^+/CH_3Cl.

[d]Derived from reaction efficiencies for methane activation by bare M^+ cations (ϕ_{CH_4}) and ammonia activation by $M(CH_2)^+$ (ϕ_{NH_3}), and branching ratios (BR) for C–N coupling, $\phi_{rel} = N \bullet \phi_{CH_4} \bullet \phi_{NH_3}(1 - BR_{NH_4^+}/100)$, with normalization constant N = 585. For M = W, Os, and Ir, ϕ_{CH_4} are taken from ref. (21); for M = Pt, ϕ_{CH_4} is the average of the values given in refs. (21) and (38).

Fe and Co (i.e., Os and Ir) react efficiently with ammonia (see below), although the release of the carbene unit is easier for 3d- than for 5d-metals [37], i.e., $D_0(Fe^+–CH_2)$ = 82 kcal/mol vs. $D_0(Os^+–CH_2)$ = 113 kcal/mol, and $D_0(Co^+–CH_2)$ = 76 kcal/mol vs. $D_0(Ir^+–CH_2)$ = 123 kcal/mol. Moreover, the fact that $Fe(CH_2)^+$ and $Co(CH_2)^+$ are able to activate several small alkanes and alkenes [49] demonstrates that these carbenes are not unreactive in general. Obviously, nucleophilic attack of the 3d-metal carbenes by ammonia is hampered compared to the higher homologs. Lack of reactivity also cannot be ascribed to a mere charge effect, because comparable theoretical calculations performed for $Fe(CH_2)^+$, $Co(CH_2)^+$, $Ni(CH_2)^+$, and their 5d-counterparts indicate that the late 3d-metal carbenes possess higher partial charges on carbon than their 5d-congeners [23,50]. Thus, the reaction of $M(CH_2)^+$ with NH_3, a rather soft nucleophile, appears to be orbital-controlled. It remains to be demonstrated whether the larger polarizabilities of the 5d-metals as well as their more effective π-bonding facilitate nucleophilic attack at the π-system and can account for the observed differences in reactivity.

The carbenes of the 4d- and 5d-metals Rh, W, Os, and Ir show moderate efficiencies in their reactions with ammonia. The major pathway in the reaction of $Rh(CH_2)^+$ and NH_3 yields Rh^+, a product channel that is not observed for platinum and the other 5d-metals. Although the neutral products cannot be detected directly, conceivable species such as $CH_2NH + H_2$ or the ylide $^–CH_2NH_3^+$ are disfavored on energetic grounds. According to thermochemical data, exothermic formation of methylamine from the couple $M(CH_2)^+/NH_3$ requires metals with $D_0(M^+–CH_2) < 87$ kcal/mol, which explains that it is only observed for $Rh(CH_2)^+$ (D_0 = 85 kcal/mol) and for none of the other 5d-metal carbenes. The formation of $CH_2NH_2^+$ and neutral MH, i.e., the main product formed from the $Pt(CH_2)^+/NH_3$ couple (Reaction 7) is not observed for rhodium; this is completely in line with thermochemical considerations that predict an endothermicity of 10 kcal/mol for this channel with this metal.

Only two reaction pathways are observed for the 5d-metal carbenes $W(CH_2)^+$ and $Ir(CH_2)^+$, i.e., dehydrogenation and an acid-base reaction to yield NH_4^+ concomitant with neutral MCH; the former presumably leads to the corresponding aminocarbenes $MC(H)NH_2^+$. Consecutively, these ions react with excess NH_3 to yield $[M,C,N_2,H_4]^+$ and molecular hydrogen. This behavior is analogous to that of the $Pt(CH_2)^+/NH_3$ couple, and we therefore tentatively assign bisaminocarbene structures $MC(NH_2)_2^+$ to these ionic reaction products. For osmium and iridium, large fractions of the carbenes are consumed by simple acid-base reactions with ammonia to afford MCH species. Conceptually, these carbyne species can be considered as precursors for soot formation such that the potential catalytic activity of these metals appears limited, judged on these particular gas-phase experiments. Although proton transfer from $M(CH_2)^+$ to ammonia is absent for tungsten, its high oxophilicity prompts efficient side reactions with background contaminants, like water or oxygen, to yield $[W,C,O,H_2]^+$ and WO_2^+, which render further investigations difficult.

The reaction of $Au(CH_2)^+$ and NH_3 yields exclusively $CH_2NH_2^+$ and neutral AuH with high efficiency; neither the acid-base reaction nor aminocarbene formation is observed. Thus, the most remarkable trend upon moving across the 5d-series concerns the decreasing branching ratio of aminocarbene vs. metal hydride formation. This trend nicely agrees with the reaction enthalpies for formation of $CH_2NH_2^+$ and neutral MH, which are negative for the late 5d-metals Ir, Pt, and Au only [47]. In fact, the above reaction is the most exothermic for gold, since $D_0(Au^+–CH_2)$ is comparatively small while the Au–H bond strength and the first ionization energy of the gold atom, terms all of which affect the reaction enthalpy, are quite large.

However, the moderate exothermicity for the $Ir(CH_2)^+/NH_3$ couple does not suffice for formation of $CH_2NH_2^+$ and IrH, and Au^+ is not capable of activating methane. Therefore, it is tempting to speculate that the unique reactivity of the platinum cation, i.e., the ability to combine methane activation with selective and efficient carbon-nitrogen coupling of the $Pt(CH_2)^+$ carbene with NH_3, is also responsible for the outstanding role of platinum as catalyst in the Degussa process to generate HCN from CH_4 and NH_3 [47,51,52].

DIRECT AMINATION AND OXYGENATION OF METHANE

Probably, the simplest and most direct access to primary amines involves the insertion of an imine fragment NH in a C–H bond of the organic substrate (Reaction 11).

$$R{-}H + NH \longrightarrow R{-}NH_2 \qquad (11)$$

However, naked imine is an energy-rich compound ($\Delta_f H$ = 90 kcal/mol), and its usually endothermic formation requires harsh conditions and high temperatures. More promising approaches involve transition metals which may serve to generate and bind the imine fragment, and eventually to transfer it to the organic substrate. In the condensed phase, a large number of transition-metal imido complexes [M](NH) are known [53–55], and depending on the electronic environment provided by [M], the reactivity character of the imine ligand can be tuned such that even activation of aliphatic and aromatic C–H bonds can be achieved. Reactivity studies of ionic $M(NH)^{+/-}$ species in the gas phase are scarce [20,56–59] due to a manifold of obstacles. From a thermochemical point of view, the bond-dissociation energy $D(M^+{-}NH)$ should be large enough to promote dehydrogenation of ammonia, i.e., $D(M^+{-}NH)$ > 101 kcal/mol. Thus, early transition metals are promising. A direct and unfortunate consequence of these high bond energies is, however, that $M(NH)^+$ ions of the early transition metals are featured by low reactivities as far as the transfer of the NH unit is concerned. The late 3d-transition-metal cations Co^+, Ni^+, and Cu^+ differ in that they do not form metal-imine complexes when reacted with NH_3 [60]. $Fe(NH)^+$ is expected to possess a well-balanced bonding situation between these extremes along the 3d-series, rendering it a suitable candidate for catalytic procedures. In fact, Freiser and coworkers have demonstrated in a pioneering study about transition-metal imines, that bare $Fe(NH)^+$ is able to transfer the imine unit to benzene as well as ethene [56]. Recently, in a detailed experimental/computational investigation Freiser's work was extended [61]. *Ab initio* calculations at the MR-ACPF level predict $Fe(NH)^+$ to have a linear sextet ground state ($^6\Sigma^+$); a bent quartet state ($^4A'$) and a linear doublet state ($^2\Delta$) are higher in energy by 0.14 eV and 0.51 eV, respectively. The bond-dissociation energy was determined to $D_0(Fe^+{-}NH)$ = 69 ± 2 kcal/mol using ion-molecule reactions, thus implying that the complex is not directly available from Fe^+/NH_3; rather reactions of bare Fe^+ with either energy-rich HN_3 or NH_2OH had to be used in the gas-phase synthesis of $Fe(NH)^+$. Interestingly, the chemical behavior of $Fe(NH)^+$ towards O_2, H_2O, H_2, benzene, toluene, and aliphatic hydrocarbons revealed an intrinsically high reactivity, and the attractive direct aminations like benzene → aniline or toluene → benzylidenimine could be afforded with high efficiencies. While ethane and propane are also converted to the corresponding amines, the reaction of $Fe(NH)^+$ with CH_4 is surprisingly inefficient (ϕ = 0.002), and also the associated kinetic isotope effect is small ($k(CH_4)/k(CD_4)$ = 1.3 ± 0.4). As stated [61], a convincing explanation for the inertness of the $Fe(NH)^+/CH_4$ couple and the distinctly different behavior of the related $Fe(NH)^+/FeO^+$ system in its reaction with H_2 and CH_4 remain to be provided by computational studies, which in view of the existence of energetically comparable spin states for $Fe(NH)^+$ will constitute a formidable challenge.

Hydroxylation of nonactivated C–H bonds is a central research issue in many areas of contemporary chemistry, and of particular interest—not least due to its economic importance—is the direct conversion of methane into methanol [1]. The efficiencies ϕ and the product branching ratios for the gas-phase reactions of methane with selected bare MO^+ cations (Reaction 12) are collected in Table 2.

$$MO^+ + CH_4 \xrightarrow{\text{(a)}} M(OH)^+ + CH_3^{\bullet} \qquad (12)$$
$$\xrightarrow{\text{(b)}} MCH_2^+ + H_2O$$
$$\xrightarrow{\text{(c)}} M^+ + CH_3OH$$

Table 2. Efficiencies (ϕ) and product-branching ratios (%) for the feactions of CH_4 with MO^+.[a]

MO^+	ϕ	$M(OH)^+/CH_3$	$M(CH_2)^+/H_2O$	M^+/CH_3OH
MnO^+	0.40	100		>1
FeO^+	0.20	57	2	41
CoO^+	0.005			100
NiO^+	0.20			100
PtO^+	1.00		75	25

[a]The data are extracted from refs. 8, 28, 38, 62, and 63.

Not unexpectedly, due to their large M^+–O bond energies the early transition-metal oxides (not included in Tabe 2) ScO^+ and TiO^+ do not react at all, and the activation of CH_4 by VO^+ hardly occurs [62,64–66]. Also of interest is a comparison of the 5d- with the corresponding 3d-transition-metal oxides. For example, PtO^+ reacts with CH_4 at the collisional limit (ϕ = 1) to yield the carbene complex $Pt(CH_2)^+$ and H_2O as predominant product [28,38], whereas the isoelectronic NiO^+ reacts five times more slowly and gives rise to Ni^+ and methanol only [36,67]. Similarly, FeO^+ oxygenates methane, while its third-row congener OsO^+ (ϕ = 0.6) exclusively dehydrogenates methane to yield $(O)Os(CH_2)^+$ [20]. The distinctly different reactivity of third-row MO^+ ions relative to their first-row analogs can partly be traced back to thermodynamic grounds, which originate from the significantly increased M^+–CH_2 bond strengths for third-row transition metals due to the operation of relativistic effects [23,24,28,68].

Of particular interest is the reaction of FeO^+ with CH_4 [69] that has been studied by three different experimental techniques, i.e., Fourier transform ion cyclotron resonance, guided ion beam, and selected-ion flow tube mass spectrometry. The peculiarities of the reactions of FeO^+ with CH_4, and also with H_2, as well as the strikingly different product distribution for different binary metal-oxide cations (see Table 2) has initiated an "explosion" of computational activities [69,71–82] that eventually resulted in a new paradigm for the metal-mediated oxygenation of hydrocarbons: the two-state reactivity (TSR) concept [77,83,84]. The essence of a TSR scenario is depicted in a simplified manner [85] in Scheme 4 for the reaction of an alkane (RH) with bare FeO^+, and the following features are worth mentioning in the present context.

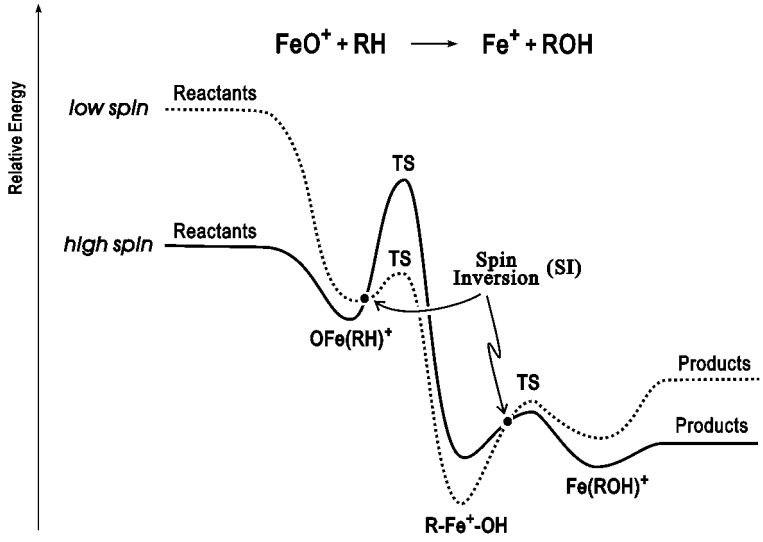

Scheme 4 Qualitative potential-energy surfaces for low- and high-spin multiplicities in the reaction of FeO^+ with a substrate RH (R = H, alkyl). TS: transition structure.

The high-spin ground-state FeO^+ ($^6\Sigma^+$) has no low-lying vacant orbitals to undergo a concerted insertion into the R–H bond, and hence, the barrier for R–H bond activation is large. In contrast, the excited, low-spin quartet states of FeO^+ ($^4\Delta$, $^4\phi$) provide high-lying doubly occupied orbitals together with low-lying empty orbitals, and thereby allow facile, concerted multi-center bond activations. In fact, not only are the barriers lower on the low-spin pathway, but also the insertion intermediate $R–FeOH^+$ is more stable than the high–spin electromer. In the former, two covalent bonds can be formed via spin pairing, while the high-spin electromer of $R–Fe–OH^+$ is characterized by a partially anti-bonding interaction. Note that TSR does not involve any initial excitation of the reactants; rather, spin inversion occurs en route to the products and thus provides an energetically more favored reaction channel. In even a more general sense, the high-spin metal-oxo species can only undergo single-bond reactions, i.e., atom abstractions, radical-type processes, or electron transfer, whereas in addition to these, the low-spin states can also promote two-bond reactions, such as concerted bond insertion. Interestingly, several anomalies (kinetic isotope effects, inverse temperature dependencies, branching ratios) in the reactions of FeO^+ with various RH substrates, e.g., molecular hydrogen [70], methane [70], benzene [87–89], norbornane [90,91], have been resolved by applying TSR, and there is also mounting evidence that the concept of two-state reactivity helps to clarify conflicting interpretations on intriguing experimental findings in the cytochrome P-450 mediated hydroxylations of hydrocarbons [83,84,92]. In addition, Yoshizawa and coworkers have demonstrated that in the hydroxylation of methane by FeO^{n+} (n = 0–2) the concerted, low-spin pathways are preferred irrespective of the actual charge state of the oxidant [76]. Most recently, the same research groups have addressed the femtosecond dynamics for the reactions of FeO^+ with both methane and benzene [93].

Reactivity enhancement by sequential ligation of the bare-metal cations has been demonstrated repeatedly, and a particularly striking example in the context of methane activation is provided by MoO_n^+ (n = 1 – 3) [94]. While MoO^+ and MoO_2^+ do not exhibit any reactivity toward CH_4, the trioxide MoO_3^+ reacts efficiently and the only products formed are $CH_3^\bullet$ (75%), CH_2O (20%), H_2O (4%), and CH_3OH (1%). Detailed experimental and computational studies [95], including labeling experiments, suggest a scenario as depicted in Scheme 5. Not surprisingly, the initial step, i.e., hydrogen atom abstraction, is typical for an oxygen-centered radical as in MoO_3^+.

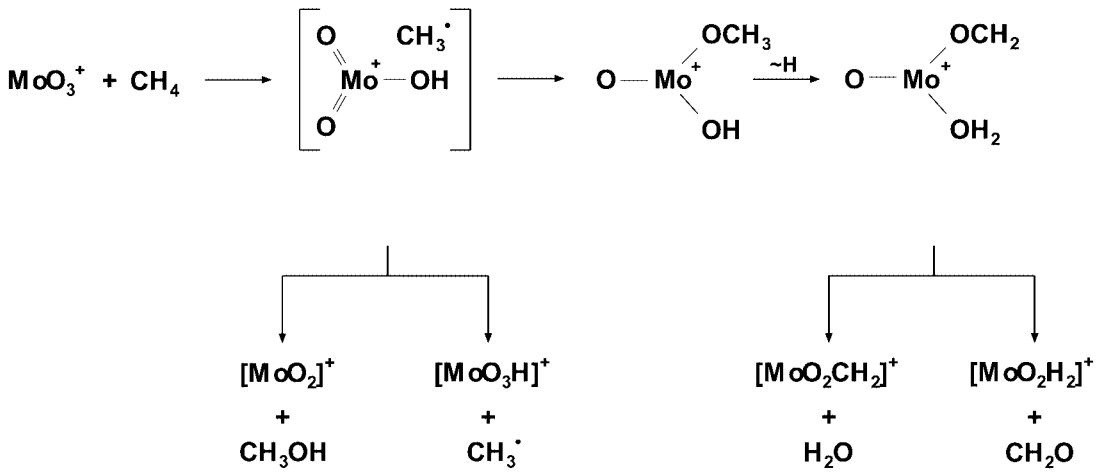

Scheme 5 Methane activation by bare MoO_3^+ (taken from ref. 94).

Similarly, CrO^+ does not react with CH_4, while the high-valent Cr(V) dioxide cation $OCrO^+$ is quite reactive ($\phi = 0.12$), and the product distribution is shown in Reaction 13 [96].

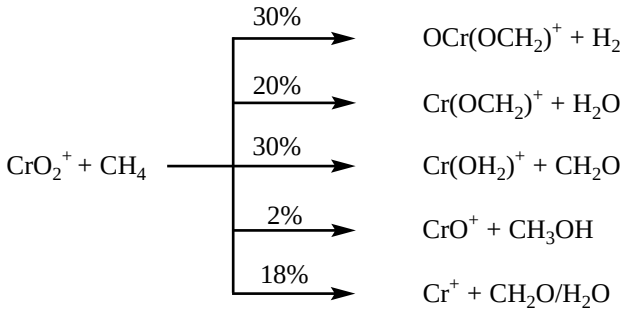

(13)

The $OCrO^+/CH_4$ couple necessarily involves spin inversion en route to product formation, because most of the products have ground states of higher multiplicities with rather large excitation energies to the doublet surface, e.g., 3.8 eV for the excitation Cr^+ (^6S) → Cr^+ (^2D). The losses of neutral H_2O, CH_2O, and "CH_4O_2" (most probably as $H_2O + CH_2O$) can be explained to proceed via the bis-ligated complex $(H_2O)Cr(OCH_2)^+$ as a common intermediate (see below). The key product corresponds to the loss of dihydrogen to yield the $[Cr,C,H_2,O_2]^+$ ion. Because previous studies have demonstrated that formaldehyde may undergo Cr^+-mediated dehydrogenation to the corresponding carbonyl complex [97,98], one is tempted to assign an analogous $(H_2O)Cr(CO)^+$ structure to this product ion and attribute its formation to a subsequent degradation of the formaldehyde ligand in $(H_2O)Cr(OCH_2)^+$. However, the secondary reaction of the $[Cr,C,H_2,O_2]^+$ product ion with background water rules out this conjecture in that formation of $[Cr,H_2,O_2]^+$ takes place; this process formally represents an exchange reaction in which water substitutes a formaldehyde ligand in $[Cr,C,H_2,O_2]^+$. These findings and extensive labeling experiments suggest that the $[Cr,C,H_2,O_2]^+$ ion indeed corresponds to a formaldehyde complex of chromium oxide, i.e., $OCr(OCH_2)^+$. At first sight, the formation of this ion is quite surprising, because it combines a reactive metal-oxo moiety with an oxidizable aldehyde ligand. However, similar reactions of only one of two oxo-ligands have been previously proposed in the reactions of OsO_2^+ with methane and CrO_2Cl^+ with ethene [20,99].

Finally, with regard to the role of high-valent metal oxides the comprehensive study of the gas-phase OsO_n^+ chemistry (n = 0–4) by Irikura and Beauchamp [20] deserves brief mentioning (Reactions 14–18).

$$Os^+ + CH_4 \xrightarrow{\phi = 0.3} Os(CH_2)^+ + H_2 \quad (14)$$

$$OsO^+ + CH_4 \xrightarrow{\phi = 0.6} Os(O)(CH_2)^+ + H_2 \quad (15)$$

$$OsO_2^+ + CH_4 \xrightarrow{\phi = 0.5} Os(O)(CH_2)^+ + H_2O \quad (16)$$

$$OsO_3^+ + CH_4 \not\longrightarrow \quad (17)$$

$$OsO_4^+ + CH_4 \xrightarrow{\phi = 0.7} Os(O)_3(OH)^+ + CH_3^\bullet \quad (18)$$

These reactions are noteworthy in that they were deemed to serve as a reactivity model for the catalytic conversion of methane into formaldehyde by metal oxides. However, the product formed in Reactions 15 and 16—in contrast to the $Cr(OCH_2)^+$ product in the related CrO_2^+/CH_4 system (Reaction 13)—corresponds to an oxo carbene complex of cationic osmium rather than $Os(OCH_2)^+$; clearly, the driving force in the osmium couples (Reactions 14–16) is the huge, relativistically stabilized Os^+–CH_2

bond energy. The nonreactivity of OsO_3^+, in contrast to the behavior of ReO_3^+ [20], is also striking. Obviously, understanding the mechanistic details of metal-oxide mediated C–H bond activation is far from being complete. As stated above, the detailed electronic structure of MO_n^+ matters a lot and the thermodynamic features of the various product channels play significant roles and need to be considered together with the origins of kinetically imposed bottlenecks [100].

ACKNOWLEDGMENTS

This research was financially supported by generous grants from the Deutsche Forschungsgemeinschaft, the Volkswagen-Stiftung, the Fonds der Chemischen Industrie, the BASF AG, the BAYER AG, and the DEGUSSA-HÜLS AG. The allocation of computer time by the Konrad Zuse Zentrum für Informationstechnik, Berlin, is appreciated. Practical and conceptual contributions by past and present members of the Berlin research group (whose names are given in the references) as well as extensive collaborations with Profs. Y. Apeloig, P. B. Armentrout, D. K. Böhme, W. Koch, S. Shaik, and P. E. M. Siegbahn and their coworkers are gratefully acknowledged.

REFERENCES AND NOTES

1. Catalytic conversion of CH_4 to CH_3OH has been listed as one of the ten challenges for catalysis: *Chem. Eng. News* **71**, 27 (May 31, 1993).
2. H. Schwarz. *Angew. Chem. Int. Ed. Engl.* **30**, 820 (1991).
3. J. M. Fox. *Catal. Rev. Sci. Eng.* **35**, 169 (1993).
4. R. H. Crabtree. *Chem. Rev.* **95**, 987 (1995).
5. G. A. Olah and A. Molnar. *Hydrocarbon Chemistry*, Wiley, New York (1995).
6. B. A. Arndtsen, R. G. Bergman, T. A. Mobley, T. H. Peterson. *Acc. Chem. Res.* **28**, 154 (1995).
7. See, for example: J. C. Weisshaar. *Acc. Chem. Res.* **26**, 213 (1993).
8. D. Schröder and H. Schwarz. *Angew. Chem. Int. Ed. Engl.* **29**, 1433 (1990).
9. L. F. Halle, P. B. Armentrout, J. L. Beauchamp. *J. Am. Chem. Soc.* **103**, 962 (1981).
10. R. Georgiadis and P. B. Armentrout. *J. Phys. Chem.* **92**, 7067 (1988).
11. M. P. Irion and A. Selinger. *Ber. Bunsenges. Phys. Chem.* **93**, 1408 (1989).
12. P. B. Armentrout and J. L. Beauchamp. *Acc. Chem. Res.* **22**, 315 (1989).
13. S. W. Buckner, T. J. McMahon, G. D. Byrd, B. S. Freiser. *Inorg. Chem.* **28**, 3511 (1989).
14. J. K. Perry, G. Ohanessian, W. A. Goddard III. *Organometallics* **13**, 1870 (1994).
15. Interesting "exceptions", based on quite different concepts, were recently reported. For example, Bowers and coworkers demonstrated that methane activation can be brought about by means of proper ligation [16]. Bondybey's laboratory reported that dimeric Rh_2^+, in distinct contrast to atomic Rh^+ as well as larger Rh_n^+ clusters, dehydrogenates CH_4 [17], and a detailed analysis of the gas-phase performance of Bergman's catalyst [6] was reported by Chen, Plattner, and their coworkers [18,19].
16. C. J. Carpenter, P. A. M. van Koppen, M. T. Bowers, J. K. Perry. *J. Am. Chem. Soc.* **122**, 392 (2000), and references therein.
17. G. Albert, C. Berg, M. Beyer, U. Achatz, S. Joos, G. Niedner-Schatteburg, V. E. Bondybey. *Chem. Phys. Lett.* **268**, 235 (1997).
18. C. Hinderling, D. A. Plattner, P. Chen. *Angew. Chem. Int. Ed. Engl.* **36**, 243 (1997).
19. C. Hinderling, D. Feichtinger, D. A. Plattner, P. Chen. *J. Am. Chem. Soc.* **119**, 10793 (1997).
20. K. K. Irikura and J. L. Beauchamp. *J. Am. Chem. Soc.* **111**, 75 (1989).
21. K. K. Irikura and J. L. Beauchamp. *J. Am. Chem. Soc.* **113**, 2769 (1991).
22. K. K. Irikura and J. L. Beauchamp. *J. Phys. Chem.* **95**, 8344 (1991).
23. C. Heinemann, R. H. Hertwig, R. Wesendrup, W. Koch, H. Schwarz. *J. Am. Chem. Soc.* **117**, 495 (1995).

24. C. Heinemann, H. Schwarz, W. Koch, K. G. Dyall. *J. Chem. Phys.* **104**, 4642 (1996).
25. D. G. Musaev and K. Morokuma, *Isr. J. Chem.* **33**, 307 (1993).
26. C. Heinemann, R. Wesendrup, H. Schwarz. *Chem. Phys. Lett.* **239**, 75 (1995).
27. J. J. Caroll, J. C. Weisshaar, P. E. M. Siegbahn, C. A. M. Wittborn, M. R. A. Blomberg, *J. Phys. Chem.* **99**, 14388 (1995).
28. M. Pavlov, M. R. A. Blomberg, P. E. M. Siegbahn, R. Wesendrup, C. Heinemann, H. Schwarz. *J. Phys. Chem. A* **101**, 1567 (1997).
29. U. Achatz, M. Beyer, S. Joos, B. S. Fox, G. Niedner-Schatteburg, V. E. Bondybey. *J. Phys. Chem. A* **103**, 8200 (1999).
30. D. G. Musaev, N. Koga, K. Morokuma. *J. Phys. Chem.* **97**, 4064 (1993).
31. D. G. Musaev, K. Morokuma, N. Koga, K. A. Nguyen, M. S. Gordon, T. R. Cundari. *J. Phys. Chem.* **97**, 11435 (1993).
32. M. R. A. Blomberg, P. E. M. Siegbahn, M. Svensson. *J. Phys. Chem.* **98**, 2062 (1994).
33. D. G. Musaev and K. Morokuma. *J. Phys. Chem.* **100**, 11600 (1996).
34. M. Hendrickx, M. Ceulemans, L. Vanquickenborne. *Chem. Phys. Lett.* **257**, 8 (1996).
35. K. Eller and H. Schwarz. *Chem. Rev.* **91**, 1121 (1991).
36. D. Schröder and H. Schwarz. *Angew. Chem. Int. Ed. Engl.* **34**, 1973 (1995).
37. B. S. Freiser (Ed.) *Organometallic Ion Chemistry*, Kluwer Academic Publishers, Dordrecht (1996).
38. R. Wesendrup, D. Schröder, H. Schwarz. *Angew. Chem. Int. Ed. Engl.* **33**, 1174 (1994).
39. Given as $\phi = k_r/k_c$ where k_r is the experimentally observed rate constant and k_c is the collision rate constant derived from capture theory [40].
40. T. Su. *J. Chem. Phys.* **100**, 4703 (1994), and references therein.
41. D. H. R. Barton. *Aldrichimica Acta* **23**, 3 (1990).
42. R. Wesendrup and H. Schwarz. *Angew. Chem. Int. Ed. Engl.* **34**, 2033 (1995), and references therein.
43. N. Sändig and W. Koch. *Organometallics* **16**, 5244 (1997).
44. N. Sändig and W. Koch. *Organometallics* **17**, 2344 (1998).
45. M. Brönstrup, D. Schröder, H. Schwarz. *Organometallics* **18**, 1939 (1999).
46. M. Aschi, M. Brönstrup, M. Diefenbach, J. N. Harvey, D. Schröder, H. Schwarz. *Angew. Chem. Int. Ed. Engl.* **37**, 829 (1998).
47. M. Diefenbach, M. Brönstrup, M. Aschi, D. Schröder, H. Schwarz. *J. Am. Chem. Soc.* **121**, 10614 (1999).
48. For the gas-phase generation of P_6, a new phosphorus allotrope, see: D. Schröder, H. Schwarz, M. Wulf, H. Sievers, P. Jutzi, M. Reiher. *Angew. Chem. Int. Ed.* **38**, 3513 (1999).
49. S. W. Buckner and B. S. Freiser. *Polyhedron* **7**, 1583 (1988).
50. M. C. Holthausen, M. Mohr, W. Koch. *Chem. Phys. Lett.* **240**, 245 (1995).
51. D. Hasenberg and L. D. Schmidt. *J. Catal.* **104**, 441 (1987).
52. A. Bockholt, I. S. Harding, R. M. Nix. *J. Chem. Soc. Faraday Trans.* **93**, 3869 (1997).
53. P. C. Schaller, C. C. Cummins, P. T. Wolczanski. *J. Am. Chem. Soc.* **118,** 591 (1996).
54. D. F. Schafer II and P. T. Wolczanski. *J. Am. Chem. Soc.* **120**, 4881 (1998).
55. P. J. Walsh, F. J. Hollander, R. G. Bergman. *J. Am. Chem. Soc.* **110**, 8729 (1988).
56. S. W. Buckner, J. R. Gord, B. S. Freiser. *J. Am. Chem. Soc.* **110**, 6606 (1988).
57. D. E. Clemmer, L. S. Sunderlin, P. B. Armentrout. *J. Phys. Chem.* **94**, 3008 (1990).
58. D. R. A. Ranatunga, Y. D. Hill, B. S. Freiser. *Organometallics* **15**, 1242 (1996).
59. T. C. Lau, Z. Wu, I. Wang, K. W. M. Sin, R. Guevremont. *Inorg. Chem.* **35**, 2169 (1996).
60. D. E. Clemmer and P. B. Armentrout. *J. Phys. Chem.* **95**, 3084 (1991).
61. M. Brönstrup, I. Kretzschmar, D. Schröder, H. Schwarz. *Helv. Chim. Acta* **81**, 2348 (1998).
62. M. F. Ryan, A. Fiedler, D. Schröder, H. Schwarz. *Organometallics* **13**, 4072 (1994).
63. M. F. Ryan, A. Fiedler, D. Schröder, H. Schwarz. *J. Am. Chem. Soc.* **117**, 2033 (1995).

64. M. M. Kappes and R. H. Staley. *J. Am. Chem. Soc.* **103**, 1286 (1981).
65. D. E. Clemmer, N. Aristov, P. B. Armentrout. *J. Phys. Chem.* **97** 544 (1993).
66. Y. M. Chen, D. E. Clemmer, P. B. Armentrout. *J. Am. Chem. Soc.* **116**, 7815 (1994).
67. See also: D. Schröder, A. Fielder, M. F. Ryan, H. Schwarz. *J. Phys. Chem*. **98**, 68 (1994).
68. K. K. Irikura and W. A. Goddard III. *J. Am. Chem. Soc.* **116**, 8733 (1994).
69. D. Schröder, A. Fiedler, J. Hrušák, H. Schwarz. *J. Am. Chem. Soc.* **114**, 1245 (1992).
70. D. Schröder, H. Schwarz, D. E. Clemmer, Y. Chen, P. B. Armentrout, V. I. Baranov, D. K. Böhme. *Int. J. Mass Spectrom. Ion Processes* **161**, 175 (1997).
71. A. Fiedler, D. Schröder, S. Shaik, H. Schwarz. *J. Am. Chem. Soc.* **116**, 10734 (1994).
72. S. Shaik, D. Danovich, A. Fiedler, D. Schröder, H. Schwarz. *Helv. Chim. Acta* **78**, 1393 (1995).
73. K. Yoshizawa, Y. Shiota, T. Yamabe. *Chem. Eur. J.* **3**, 1160 (1997).
74. D. Danovich and S. Shaik. *J. Am. Chem. Soc.* **119**, 1773 (1997).
75. K. Yoshizawa, Y. Shiota, T. Yamabe. *J. Am. Chem. Soc.* **120**, 564 (1998).
76. K. Yoshizawa, Y. Shiota, T. Yamabe. *Organometallics* **17**, 2825 (1998).
77. K. Yoshizawa, Y. Shiota, T. Yamabe. *J. Chem. Phys.* **111**, 538 (1999).
78. A. Irigoas, J. M. Ugalde, X. Lopez, C. Sarasola. *Can. J. Chem.* **74**, 1824 (1996).
79. A. Irigoas, J. E. Fowler, J. M. Ugalde. *J. Phys. Chem. A* **121**, 2252 (1998).
80. A. Irigoas, J. E. Fowler, J. M. Ugalde. *J. Am. Chem. Soc.* **121**, 574 (1999).
81. A. Irigoas, J. E. Fowler, J. M. Ugalde. *J. Am. Chem. Soc.* **121**, 8549 (1999).
82. A. Irigoas, D. Eliszalde, I. Silanes, J. E. Fowler, J. M. Ugalde. *J. Am. Chem. Soc.* **122**, 114 (2000).
83. S. Shaik, M. Filatov, D. Schröder, H. Schwarz. *Chem. Eur. J.* **4**, 193 (1998).
84. D. Schröder, S. Shaik, H. Schwarz. *Acc. Chem. Res.* **33**, 139 (2000).
85. For more detailed treatments, see refs. 72, 74, 77, 83, 84, and 86.
86. M. Filatov and S. Shaik. *J. Phys. Chem. A* **102**, 1281 (1992).
87. D. Schröder and H. Schwarz. *Helv. Chim. Acta* **75**, 1281 (1992).
88. H. Becker, D. Schröder, H. Schwarz. *J. Am. Chem. Soc.* **116**, 1096 (1994).
89. K. Yoshizawa, Y. Shiota, T. Yamabe. *J. Am. Chem. Soc.* **121**, 147 (1999).
90. J. Schwarz and H. Schwarz. *Helv. Chim. Acta* **78**, 1013 (1995).
91. N. Harris, S. Shaik, D. Schröder, H. Schwarz. *Helv. Chim. Acta* **82**, 1784 (1999).
92. P. H. Toy, M. Newcomb, P. F. Hollenberg. *J. Am. Chem. Soc.* **120**, 7719 (1998).
93. K. Yoshizawa, Y. Shiota, Y. Kagawa, T. Yamabe. *J. Phys. Chem.* **104**, 2552 (2000).
94. C. J. Cassady and S. W. McElvany. *Organometallics* **11**, 2367 (1992).
95. I. Kretzschmar, A. Fiedler, J. N. Harvey, D. Schröder, H. Schwarz. *J. Phys. Chem. A* **101**, 6252 (1997).
96. A. Fiedler, I. Kretzschmar, D. Schröder, H. Schwarz. *J. Am. Chem. Soc.* **118**, 9941 (1996).
97. A. Schalley, R. Wesendrup, D. Schröder, H. Schwarz. *J. Am. Chem. Soc.* **117**, 7711 (1995).
98. R. Wesendrup, C. A. Schalley, D. Schröder, H. Schwarz. *Chem. Eur. J.* **1**, 608 (1995).
99. D. M. Walba, C. H. DePuy, J. J. Grabowski, V. M. Bierbaum. *Organometallics* **3**, 498 (1984).
100. For a detailed discussion of selected high-valent di- and trioxides of cationic transition metals, see: D. Schröder, H. Schwarz, S. Shaik. In *Structure and Bonding*, B. Meunier (Ed.), p. 97, Springer Verlag, Berlin, Heidelberg (2000).